Ring Inversion in 1,4,7 Cyclononatriene and Analogues: *Ab Initio* and DFT Calculations and Topological Analysis

MIGUEL A. ZAMORA, FERNANDO D. SUVIRE, RICARDO D. ENRIZ
Departamento de Química, Universidad Nacional de San Luis, Chacabuco 917, 5700 San Luis, Argentina

Received 9 February 2007; Revised 8 May 2007; Accepted 9 May 2007
DOI 10.1002/jcc.20789
Published online in Wiley InterScience (www.interscience.wiley.com).

Abstract: The multidimensional conformational potential energy hypersurfaces (PEHSs) for *cis-cis-cis* 1,4,7 cyclononatriene (**I**), Tribenzocyclononatriene (TBCN) (**II**), and *cis-cis-cis* cyclic triglycine (**III**) were comprehensively investigated at the Hartree–Fock (HF/6-31G(d)) and density functional theory (B3LYP/6-31G(d,p)) levels of theory. The equilibrium structures, their relative stability, and the transition state (TS) structures involved in the conformational interconversion pathways were analyzed. Altogether, four geometries (two low-energy conformations and two transition states) were found to be important for a description of the conformational features of compounds **I–III**. B3LYP/aug-cc-pvdz//B3lYP/6-31G(d,p) and MP2/6-31G(d,p)//B3LYP/6-31G(d,p) single point calculations predict that the conformational interconversion between crown and twist forms requires 14.01, 26.71, and 17.79 kcal/mol for compounds **I**, **II**, and **III**, respectively, which is in agreement with the available experimental data. A topological study of the conformational PEHSs of compounds **I–III** was performed. Our results allow us to form a concise idea about the internal intricacies of the PEHSs of compounds **I–III**, describing the conformations as well as the conformational interconversion process in these hypersurfaces.

 J Comput Chem 00: 000–000, 2007

Key words: cyclononatriene; tribenzocyclononatriene; cyclic-tryglicine; ring inversion; *ab initio*; DFT calculations

Introduction

The knowledge of conformational behavior is expected to provide insight into biologically important phenomena such as molecular recognition. Though structural data can be obtained from NMR and X-ray diffraction, reliable interpretations of experimental data can be better achieved using theoretical methods.[1] Conformational space exploration is a difficult problem, especially for cyclic molecules because of the interdependence of torsional angles.[2] For systems with numerous degrees of freedom, the potential energy hypersurface (PEHS) may have a substantial number of local minima as well as transition states (TS) interconnecting these minima. Therefore, to determine all the critical points is not an easy task.[3] Furthermore, finding the global minimum energy conformation alone may not be sufficient. It might be tempting to assume that the conformers missed, with some particular search method, are likely to be either high in energy or kinetically very unstable and thus less significant. However, it is more prudent to locate all the possible critical points on an energy hypersurface first and then, to examine their stability and their ease of conversion to other conformers to determine their relative importance. It is clear that this is a problem of considerable computational magnitude, even for relatively simple acyclic molecules. This problem becomes even more complex when partially flexible rings are involved.

We recently reported a comprehensive conformational study of cyclononane PEHS using *ab initio* and DFT calculations.[4] Our results showed that the PEHS of this apparently simple molecule is very complex. Fortunately, the PEHS of *cis-cis-cis*-1,4,7-cyclononatriene (**I**) (Fig. 1) appears to be a little more simple. *cis-cis-cis*-1,4,7-cyclononatriene (**I**) and structurally related compounds show some unusual conformational properties.[5–20] The ring system can exist in either a crown (C), which is rigid and has C_{3v} symmetry for the parent hydrocarbon, or as a "saddle" conformation, which is more or less flexible. In later sections we will discuss whether "saddle" is an appropriate name for this conformer. Both types of conformations (crown and "saddle") have been observed in the cyclotriveratrilene (CTV) series[17–20] and are separated by relatively high barriers (≈25 kcal/mol), thus giving rise to atropisomers.

Numerous theoretical and experimental studies have been carried out on **I**. However, in spite of the accumulation of a significant

Correspondence to: R.D. Enriz; e-mail: denriz@unsl.edu.ar

Contract/grant sponsor: Universidad Nacional de San Luis (UNSL)

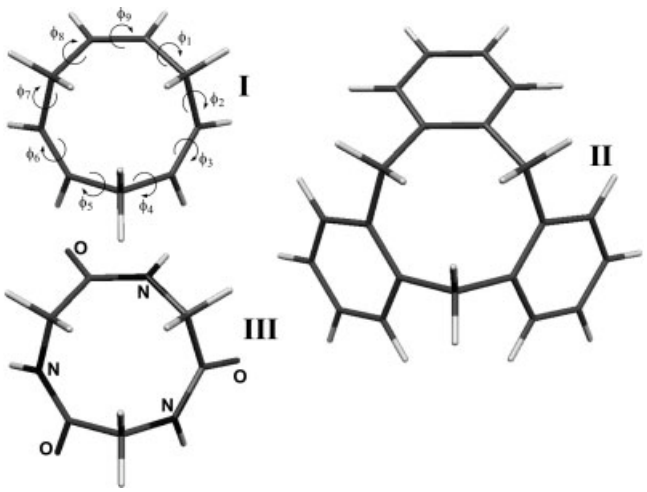

Figure 1. Structure of compounds **I–III** showing the torsional angles. The peptide bonds are also shown in compound **III**.

amount of data collection, a TS structure, as well as the complete topology involved in the ring inversion of **I** has been overlooked. Thus, the complete PEHS of **I** showing the geometries and energies of the different critical points has not been reported yet.

Tribenzocyclononatriene (TBCN) represented by the general structure **II** (Fig. 1) is an important core structure around which molecular receptors have been constructed for studying molecular recognition.[18] Cyclotriveratrylene (CTV) is the parent compound of many homologous series based on the TBCN core. These compounds have gained considerable interest throughout the years because of their special (crown/saddle) conformational isomerism,[18–20] structural chirality,[17,18,21,22] tendency to form molecular complexes[23,24] and their mesomorphic properties.[14,25,26] Different TBCN derivatives have been previously obtained through elaborate synthetic methodologies. Chakrabarti et al. synthesized in moderate yields a CTV by the acid catalyzed condensation of 3,4-dimethoxibenzyl-alcohol[27] by a modified recrystalization procedure.[28] Closely related to **I**, the TBCN core can acquire two energy-minimum conformations, a rigid crown and a more flexible "saddle". In most derivatives of TBCN the "saddle" form is less stable than the crown, and it has been estimated that the "saddle" conformation is at least 2.86–3.82 kcal/mol higher in energy than the crown isomer.[29] However, when the cyclononatriene ring is perturbed, for example when the ortho positions in the benzene rings are substituted with bulky groups, then the "saddle" form is stabilized with respect to the corresponding crown conformation. The two isomers then coexist in solution in thermal equilibrium.[19] Interestingly, the "saddle" conformation has been recently isolated and characterized through thermal isomerization by Zimmerman et al.[20] It is well known[18–20] that the crown form of TBCN and CTV can undergo inversion in which the crown core is inverted into its reflected structure. However, the complete PEHS of TBCN showing the geometries of different critical points has not been reported yet.

Like TBCN, cyclic peptides are also attractive candidates for artificial receptors because they have a rigid peptide backbone that forms a cavity and provides binding sites suitable for guest molecules. *N*-methylated cyclic triglicine has a C_3 symmetry conformation (crown form) elucidated by NMR[30,31] and X-ray crystallography studies.[32] Hioki et al.[33] reported the synthesis of N-substituted cyclic triglycines using *N*,*N*′,*N*″-triallyl-cyclo-triglicine as a scaffold. The ^{1}H and ^{13}C NMR spectra of this compound indicate that the major conformation was the crown form along with some "saddle" form (they called it boat). We focused on the *cis-cis-cis* cyclic triglicine (**III**) (Fig. 1) because it could display a closely related PEHS to those of compounds **I** and **II**.

In the early days of conformational analysis, only symmetrical conformations of the medium-ring-cycloalkanes and derivatives were thought to be local minima or even TSs for conformational interconversion,[34] but this proved not to be the case.[35,36] Nowadays, it is well known that energy minima have to be carefully distinguished from TSs in the PEHS. Extensive searches of the conformational energy hypersurface for local minima should include the barriers separating pairs of conformations. The conformational analysis of **I, II,** and **III** has been synonymous with a search for low-energy minima on the PEHS either because it is more difficult to locate saddle points than local minima or because the importance of saddle points has simply not been well appreciated. Progress in searching for TSs and their significance is likely to be much more demanding in computer time than simply searching for local energy minima because it is not sufficient just to locate the saddle points on the PEHS. It is also necessary to find out how the low energy minima and the TSs are linked together, and this requires an exploration of a larger part of the hypersurface. Compounds **I–III** only have two low-energy conformations on their PEHSs; but, where does one form change to the other and how far from an energy minimum can the molecule stray away before ceasing to be in the other conformation? In principle, the concept of structure is more general than the concept of geometry. The minimum is a low-energy point corresponding to a fixed geometry. However, the geometry may be distorted away from that point and still be regarded as the same structure. It will remain the same structure, no matter how distorted it may be until it passes through an adjacent TS to the next structure. It is clear, therefore, that information about the local and the global minimum of molecules such as **I–III** is not enough. We need to have at least a good idea of the shape and also some indication about the dynamic behavior of the internal degree of freedom of these compounds. A full understanding of the PEHS requires identification of the complete network of conformational interconversions among the different critical points.

We report here an exhaustive conformational analysis of compounds **I–III** using *ab initio* and density functional theory (DFT) computations. Besides the conformers populations, it is of great interest to know how the interconversions between the conformers are, and which of them occurs most readily. The equilibrium structures, their relative stability, and the TS structures involved in the conformational interconversion pathways were analyzed. Thus, we report here the PEHSs of molecules **I**, **II,** and **III**, including the determination of all critical points geometries. The PEHSs topological aspects are also discussed in this paper.

Table 1. Relative Energies for the Different Critical Points of Compounds **I**, **II**, and **III** Obtained From RHF/6-31G(d) and B3LYP/6-31G(d,p) Optimizations and B3LYP/Aug-cc-pvdz//B3LYP/6-31G(d,p) and MP2/6-31G(d,p)//B3LYP/6-31G(d,p) Single Point Calculations.

Compounds	Conf.	RHF/6-31G(d) ΔE (kcal/mol)	B3LYP/6-31G(d,p) ΔE (kcal/mol)	B3LYP/Aug-cc-pvdz// B3LYP/6-31G(d,p) ΔE (kcal/mol)	MP2/6-31G(d,p)// B3LYP/6-31G(d,p) ΔE (kcal/mol)
I	C	0.00	0.00	0.00	0.00
	T	3.22	2.61	2.96	3.24
	$TS_{C\text{-}T}$	16.26	14.30	14.01	18.14
	$TS_{T\text{-}T}$	4.61	3.96	3.93	5.03
II	C	0.00	0.00	0.00	0.00
	T	2.91	2.28	2.32	2.75
	$TS_{C\text{-}T}$	30.92	27.11	26.71	30.77
	$TS_{T\text{-}T}$	5.64	4.70	4.05	5.43
III	C	0.0	0.00	0.00	0.00
	T	2.15	2.54	2.87	2.07
	$TS_{C\text{-}T}$	17.99	17.10	17.79	18.35
	$TS_{T\text{-}T}$	5.75	5.19	4.94	5.62

Calculations

All the calculations reported here were performed using the GAUSSIAN 03 program.[37] Critical points (low-energy conformations and TS structures) were optimized at RHF/6-31G(d) and B3LYP/6-31G(d,p) levels of theory. An extensive search to localize first-order saddle points on the PEHSs was carried out first by using starting geometries suggested by GASCOS algorithm.[38] These input files were used to obtain the TS structures using both RHF/6-31G(d) and B3LYP/6-31G(d,p) calculations. Vibrational frequencies for the optimized structures were computed to evaluate the zero-point energies (ZPE) as well as to confirm the nature of the singular points along the potential energy surface. The stationary points have been identified as a minimum with no imaginary frequencies, or as a first-order TS characterized by the existence of only one imaginary frequency in the normal mode coordinate analysis. TS structures were located until the Hessian matrix had only one imaginary eigenvalue, and the TSs were also confirmed by animating the negative eigenvectors coordinate with a visualization program and internal reaction coordinate (IRC) calculations.[39,40] B3LYP/6-31G(d,p) IRC calculations were performed on the TS structures to check that the TSs structures lead to the initial conformer and to the final conformation (forward and reverse directions of the conformational interconversion path). IRC calculations were carried out along the path in cartesian coordinates in six points forward and six points in the reverse direction, in steps of 03 amu$^{1/2}$ bohr.

DFT calculations were employed to properly account for the electron correlation effects. Thus, the widely employed hybrid method denoted by B3LYP[41–43] was used, along with the double-seta-split valence basis set 6-31G(d,p). This method includes a mixture of Hartree–Fock (HF) and DFT exchange terms and the gradient corrected correlation functional of Lee et al.[44] and Miehlich et al.[45] as proposed and parameterized by Becke.[46,47] After obtaining these optimized structures, the most reliable, flexible basis set (aug-cc-pvdz) and MP2/6-31G(d,p) single point calculations on these geometries were used to evaluate the energies.

Results and Discussion

PEHS of cis-cis-cis-*1,4,7 Cyclononatriene (I), Tribenzocyclononatriene (TBCN) (II), and* cis-cis-cis *Cyclic Triglycine (III)*

PEHS of cis-cis-cis-*1,4,7 Cyclononatriene (I)*

The GASCOS algorithm combined with *ab initio* and DFT optimizations permits to search the PEHS for the two minimum-energy conformations as well as two transition structures connecting these conformations. The search located the two previously reported structures (C and T) together with two TSs ($TS_{C\text{-}T}$ and $TS_{T\text{-}T}$). It should be noted that although Anet and Giachi[13] reported a distorted structure of $TS_{C\text{-}T}$, the other TS structure was not found by earlier searching techniques, at least to our knowledge. The four geometries (two low-energy conformations and two TSs) were found to be important for a description of **I** conformational intricacies.

All the levels of theory reported here indicate that the most stable conformation of **I** is the crown form (C) (Table 1). It should be noted that the energy obtained for the crown from B3LYP/aug-cc-pvdz//B3LYP/6-31G(d,p) calculations is a little lower than that previously reported by Palmer and Nisbet[16] (−346.85156 au) using a Dunning double zeta basis. The structure of **I** in the crystal at −35°C has been previously determined to be a crown by X-ray diffraction analysis. Both levels of calculations, RHF/6-31G(d,p) and B3LYP/6-31G(d,p), well reproduce the bond distances and angles observed at X-ray even when periodical conditions were not considered in our calculations. The torsional angles of all the stationary points optimized at the B3LYP/6-31G(d,p) level of theory are given in Table 2.

The other low-energy conformation of **I** is the previously called "saddle" form. This conformation, however, is not a symmetric (C_S) structure but a twisted conformation, and therefore, it is more convenient to call it twisted form (T). This conformation acquires a twisted spatial ordering to reduce the repulsive interaction between the inner methylene hydrogens. The T conformation has more angle bending strain than does the C, and

Table 2. Torsional Angles and Frequency Values Obtained for the Different Critical Points of Compounds **I**, **II**, and **III** From B3LYP/6-31G(d,p) Calculations.

Compound	Conf.	ϕ_1 (°)	ϕ_2 (°)	ϕ_3 (°)	ϕ_4 (°)	ϕ_5 (°)	ϕ_6 (°)	ϕ_7 (°)	ϕ_8 (°)	ϕ_9 (°)	Frequencies (cm^{-1})
I	C	91.73	−91.73	0.00	91.73	−91.73	0.00	91.73	−91.73	0.00	159.806
	T	55.83	−103.08	−3.06	34.97	34.88	−3.05	−103.06	55.85	1.10	31.019
	TS_{C-T}	98.69	−66.97	−1.94	20.99	−20.95	1.89	66.96	−98.66	0.00	−111.946
	TS_{T-T}	81.67	−81.63	2.26	−25.01	87.69	0.01	−87.64	24.94	−2.26	−75.325
II	C	94.67	−94.70	0.09	94.54	−94.56	−0.19	94.75	−94.52	−0.06	41.513
	T	61.87	−105.70	−6.12	31.13	41.52	−7.62	−106.97	59.79	1.74	16.242
	TS_{C-T}	106.51	−64.87	−1.35	3.12	−3.13	1.36	64.88	−106.51	0.00	−163.051
	TS_{T-T}	89.09	−89.43	4.95	−33.09	93.49	−0.15	−93.52	33.28	−4.71	−38.929
III	C	89.16	−99.13	9.14	89.04	−99.16	9.70	88.33	−99.15	9.48	55.498
	T	47.58	−102.85	0.37	24.13	56.28	−22.42	−99.49	55.65	12.26	35.380
	TS_{C-T}	98.66	−43.01	37.55	−13.05	−72.56	49.15	75.61	−87.26	−44.06	−184.033
	TS_{T-T}	91.96	−78.80	−9.49	−21.32	84.63	9.46	−94.52	30.77	−10.13	−61.281

this causes it to be 2.61 kcal/mol less stable than the crown at B3LYP/aug-cc-pvdz//B3LYP/6-31G(d,p) level. Because of its rigidity and the presence of a threefold real symmetry axis, the crown has lower entropy than the Twist. However, these entropy effects are sufficiently small so that the crown should be favored in its equilibrium with the twist, and thus, only the crown is expected to be significantly populated in agreement with all experimental data. In total there are six degenerated T conformers in the PEHS (more details about this situation will be discussed at the end of this section and its topological aspects will be analyzed in the next section).

If only one methylene group is movement, then the crown (C) becomes less symmetrical through the TS TS_{C-T} and then is converted to the symmetrical saddle structure (TS_{T-T}) which is rapidly converted into the twist form (T) (Fig. 2). The energy of TS_{C-S} relative to that of the crown is 14.01 kcal/mol, a value which is in complete agreement with the observed NMR barrier (activation energy of 14.6 kcal/mol).[8] This TS structure for ring interconversion in compound **I** has two adjacent double bonds located with an ideal geometry for hyper-conjugation with the methylene groups as shown in Figures 2 and 3. The effect of an adjacent π system should be to stabilize the linear state more than the tetrahedral state because of increased hyperconjugation. Thus, the energy required to distort a tetracoordinate carbon from tetrahedral to linear should be lowererd by the presence of adjacent π orbitals. This situation might be appreciated in Figure 3. A similar but someone distorted structure was reported by Anet and Ghiachi[13] using the Boyd Force field. However, the energy for ring inversion was overestimated in 24 kcal/mol. The authors predict that this problem could be better explained using more accurate *ab initio* calculations. It is clear that hyper-conjugative and/or hybridization effects which have not been included in the force-field calculations[48–50] might be the principal responsible for such overestimation. An examination of this TS geometry shows the presence of some extraordinarily large bond angles. One C—CH_2—C angle has the value of 134°. Thus, the opening of a C—CH_2—C angle ultimately results in an almost linear carbon arrangement (Figs. 2 and 3). Species geometries along the lowest energy pathway computed at B3LYP/6-31G(d,p) illustrated in Figures 2 and 4 are informative.

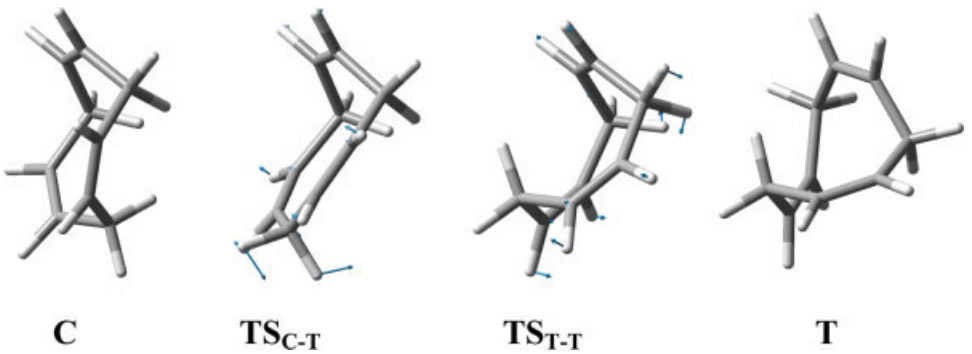

Figure 2. Optimized structures of low-energy forms and transition states of compound **I** in the lowest energy pathway at B3LYP/6-31G(d,p) level of theory. The result of the vibrational analysis of the transition states is also shown. The length of each arrow is proportional to the degree of vibration of the atom. [Color figure can be viewed in the online issue, which is available at www.interscience.wiley.com.]

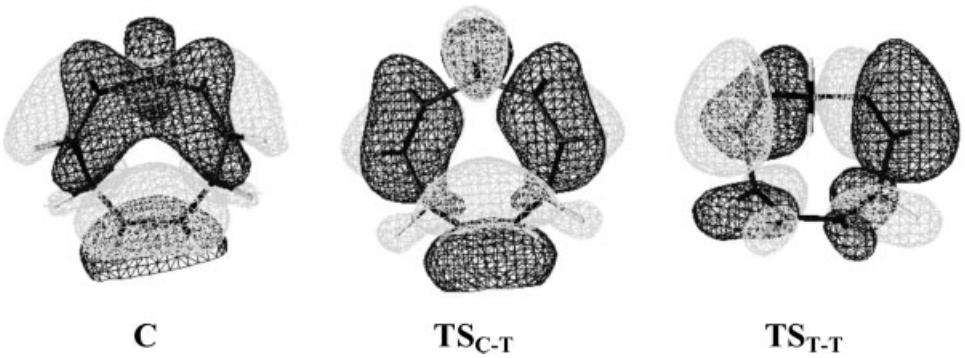

Figure 3. HOMO distribution on full optimized C, TS_{C-T}, and TS_{T-T} conformations of compound **I**. Calculations were carried out at B3LYP/6-31G(d,p) level. Note that the C form has not nodal plane at the methylene groups. TS_{T-T} displays only one nodal plane; whereas TS_{C-T} shows two nodal planes.

Starting from the symmetrical TS_{T-T} form there are two paths for the twist–twist interconversion. This process can be most simply explained by the simultaneous movement of two adjacent methylene groups. In this case the TS_{T-T} is the TS interconnecting two enantiomeric twist forms. The energy of TS_{T-T} relative to the T is only 2.5 kcal/mol at B3LYP/aug-cc-pvdz//B3LYP/6-31G(d,p) level of theory. Therefore, the barrier separating these minima is low, and hence the interconversion between these forms occurs without a significant energetic requirement. These results are in complete agreement with the experimental data previously reported by Zimmerman et al. for the saddle form of CTV derivatives. This movement gives two T structures corresponding to a right (T(R)) and a left (T(L)) twist form. It should be noted that TS_{T-T} is a highly symmetric structure possessing a characteristic saddle form (Figs. 3 and 4). The characterization of TS_{T-T} showed that the structure has only one negative eigenvalue. The calculated vibrational frequency (-75.325 cm^{-1} at B3LYP/6-31G(d,p) level) showed that the eigenvector of the imaginary frequency corresponds to the movement of two methylenes. This result might be well appreciated in Figure 4. From this TS the molecule moves down the potential energy surface to produce either the right or the left twist form.

The other path requires the movement of only one methylene group. In this case a twist form is connected through the "opposite" saddle form ($TS_{T-T(o)}$) with its enantiomeric twist-form. The characterization of the twist form showed that this form is a true minimum with no imaginary frequencies; however, it should be noted that the lowest vibrational mode corresponds to the movement of only one methylene which gives the $TS_{T-T(o)}$ form.

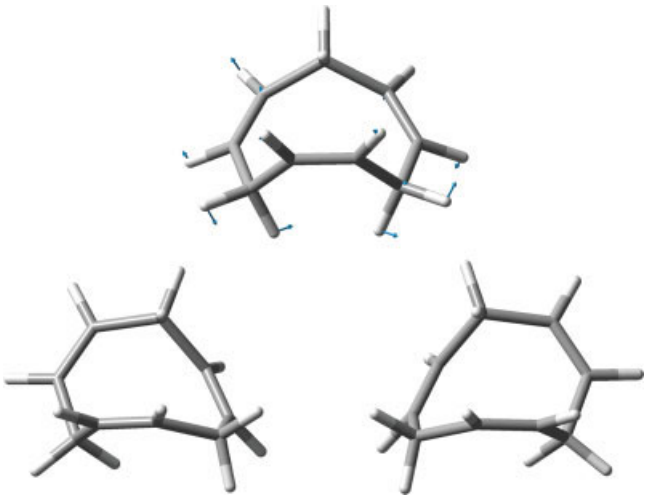

Figure 4. Optimized structures for the $T/TS_{T-T}/T$ conformational interconversion of compound **I** at B3LYP/6-31G(d,p) level. The result of the vibrational analysis (imaginary mode) of TS_{T-T} is also shown. The length of each arrow is proportional to the degree of vibration of the atom. [Color figure can be viewed in the online issue, which is available at www.interscience.wiley.com.]

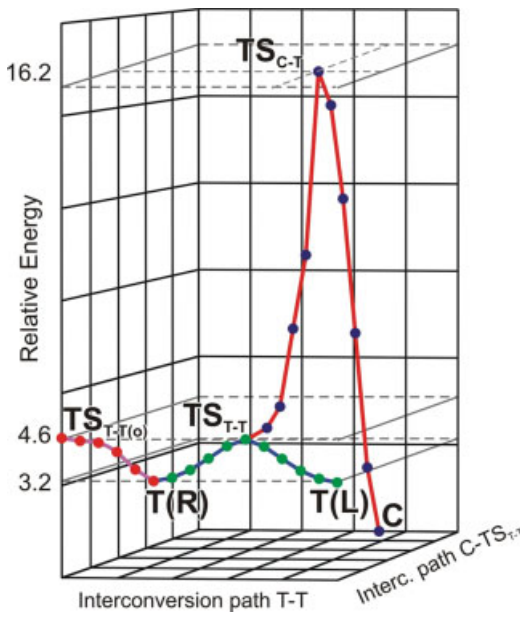

Figure 5. Two dimensional reaction path following the different conformational interconversion processes. From the TS structures, five RHF/6-31G(d) calculations were performed in forward and reverse directions. [Color figure can be viewed in the online issue, which is available at www.interscience.wiley.com.]

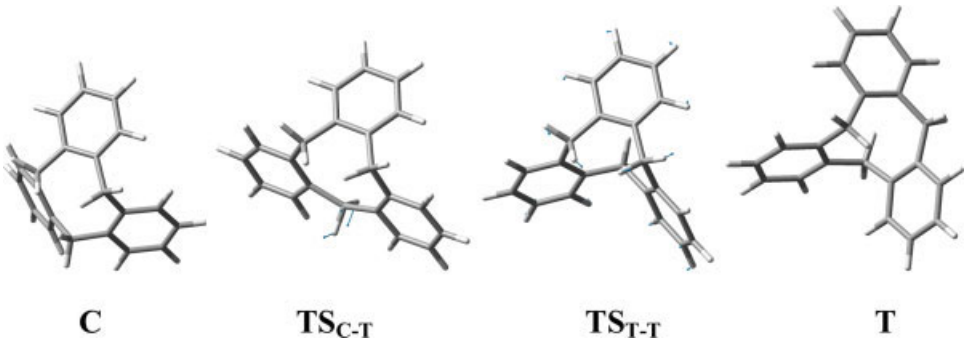

Figure 6. Optimized structures of low-energy forms and transition states of compound **II** in the lowest energy pathway at B3LYP/6-31G(d,p) level of theory. The result of the vibrational analysis of the transition states is also shown. The length of each arrow is proportional to the degree of vibration of the atom. [Color figure can be viewed in the online issue, which is available at www.interscience.wiley.com.]

By "opposite" saddle form, we mean the TS_{T-T} form obtained from the conformational interconversion of the inverse crown. Both interconversion processes allow the complete conformational interconversion among all the twist forms. Thus, each twist form is connected with other two twist forms (see later section).

To obtain a clear profile of the overall conformational process in **I**, it is necessary to underline the role of the TS_{T-T} form. This critical point is a true TS with the two levels of theory reported here. Thus, on the basis of our results we have no doubt about the character of a typical saddle point of TS_{T-T}. However, this critical point appears to play a significant role in all the conformational interconversion processes. TS_{T-T} is a typical TS structure connecting enantiomeric twist forms whereas in the crown-twist interconversion process, TS_{T-T} appears to be an inflection point between the crown and the twist conformations. Inflection points can be associated with any PEHS if the geometrical conditions are suitable, and such conditions may not be rare. For example, an inflection point may be generated from a double minimum energy surface having a small barrier separating the two minima. On the other hand, a local energy minimum that has a very low frequency vibration (as well as a TS possessing a small negative frequency) is an indication that the energy surface requires careful examination. Thus, to obtain a better description of this section of the PEHS, we performed RHF/6-31G(d,p) calculations following both interconversion processes: $C/TS_{C-T}/T$ and $T/TS_{T-T}/T$. As the construction of a complete potential energy surface would be practically impossible, we analyze the minimum-energy paths to get detailed information about the dynamics. These results are shown in Figure 5 and give an additional support for the role played by TS_{T-T} form in these processes.

It should be noted that the curve shown in Figure 5 display two adjacent TSs. The analysis of this particular zone of the PEHS of compound **I** requires a this point an extra coment. A "monkey saddle" type degenerate saddle point belongs to three critical points energy paths. These paths may also be interpreted as one path originating from one critical point and branching into two paths at the saddle point yielding two minima.[51]

The zone of a surface involving two adjacent TSs has been called as valley-ridge inflection point.[52–56] For recent discussion of valley-ridge inflection points see refs. 54–56. Unfortunately, selectivity in the area of the valley-ridge inflection of Figure 5 cannot be analyzed using TS theory. Without a barrier, TS theory simply does not apply, and a dynamic approach is required. Thus, in principle from the calculations reported here we cannot discard the possibility of an artifact of the calculation methods. However Singleton et al.[54] have provided a experimental support for a reaction surface involving two adjacent TSs. Also, from the growing number of theorically predicted cases, there is no reason to think that surfaces involving adjacent saddle points (like here) should be rare.

PEHS of Tribenzocyclononatriene (TBCN) (II)

The results obtained for compound **II** are closely related to those attained for compound **I**. These results are summarized in Tables 1 and 2 and Figures 6 and 7. Geometries of critical points along

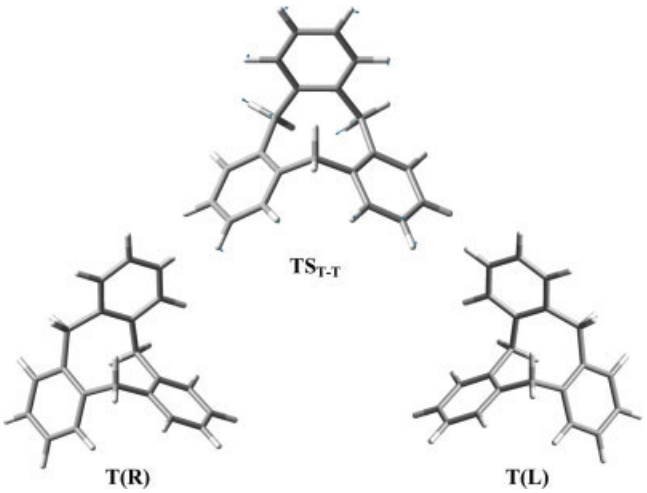

Figure 7. Optimized structures for the $T/TS_{T-T}/T$ conformational interconversion of compound **II** at B3LYP/6-31G(d,p) level. [Color figure can be viewed in the online issue, which is available at www.interscience.wiley.com.]

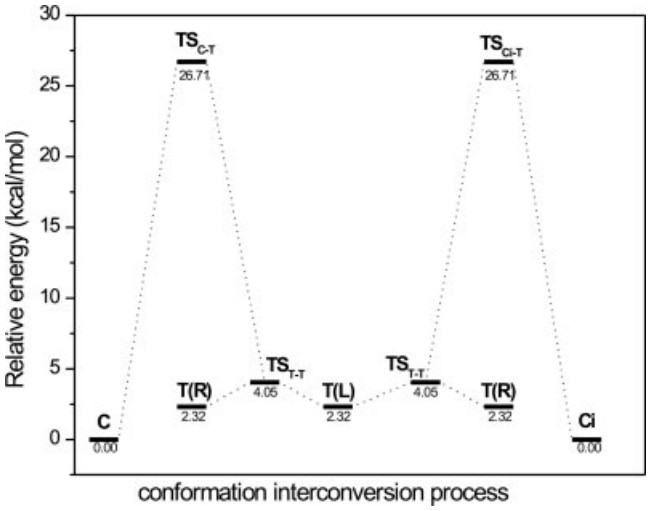

Figure 8. Schematic potential energy profile for the least energy pathway of compound **II** with relative potencial energy of conformations and transition states with respect to the global minimum. Numbers are at the B3LYP/Aug-cc-pvdz//B3LYP/6-31G(d,p) level of theory.

the lowest energy pathway computed at the B3LYP/6-31G(d,p) level are given in Figures 6 and 7. The relative energy profiles of the crown/crown, crown/twist, and twist/twist interconversions are given in Figure 8. B3LYP/aug-cc-pvdz//B3LYP/6-31G(d,p) calculations predict the crown form as the highly preferred conformation of **II**. The twist conformation possesses an energy gap of 2.32 kcal mol above the crown form. Our calculations predict that the conformational interconversion between twist forms requires only 1.73 kcal/mol which is in reasonable agreement with the results obtained by Zimmerman et al.[20] for CTV derivatives.

We also evaluated the Twist-Crown equilibrium and its interconversion kinetics in order to compare our results with those experimental data previously reported by Zimmerman et al. for cyclotriveratrylene.[20]

We quantitatively determined the equilibrium constant (T = 298 K) according to their activation energies as follows:

$$K = \exp\frac{E_{a2} - E_{a1}}{RT}$$

Where E_{a1} is the activation energy of C form and E_{a2} is the activation energy of T form. These results are shown in Table 3.

Table 3. Activation Energies and Equilibrium Constants for the Conformational Interconversions of Compounds **I–III** Obtained from B3LYP/6-31G(d,p) Calculations.

Compound	E_{a1}	E_{a2}	K
I	13.70543499	11.23869515	0.015515688
II	25.79126796	23.69413121	0.028963846
III	16.4608292	14.11268865	0.018956477

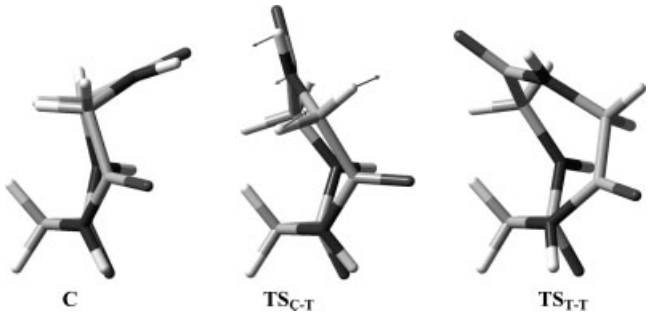

Figure 9. B3LYP/6-31G(d,p) optimized geometries of the C, $TS_{C\text{-}T}$ and $TS_{T\text{-}T}$ forms of compound **III**. The vibrational modes are shown in the $TS_{C\text{-}T}$ transition state structure.

Our results are intermediate values in comparison with those obtained by Zimmerman et al. using chloroform (K (300 K) = 0.1) and dimethylformamide (K (300 K) = 0.008). Considering that our results are obtained in gas phase they are in good agreement with the experimental data.

PEHS of cis-cis-cis *Cyclic Triglycine (III)*

As we expected, the results obtained for compound **III** are closely related to those attained for compounds **I** and **II**; only some differences were observed for the crown-twist interconversion process.

The crown form is the highly preferred conformation of **III**, being the twist form the local minimum having 2.87 kcal/mol above the global minimum (Table 1). Figure 9 shows the conformational C/$TS_{C\text{-}T}$/S interconversion geometries whereas Figure 10 gives the T/$TS_{T\text{-}T}$/T process. It is interesting to note that compound **III**, in contrast to compounds **I** and **II**, performs its C-T interconversion through the inversion of the peptide plane

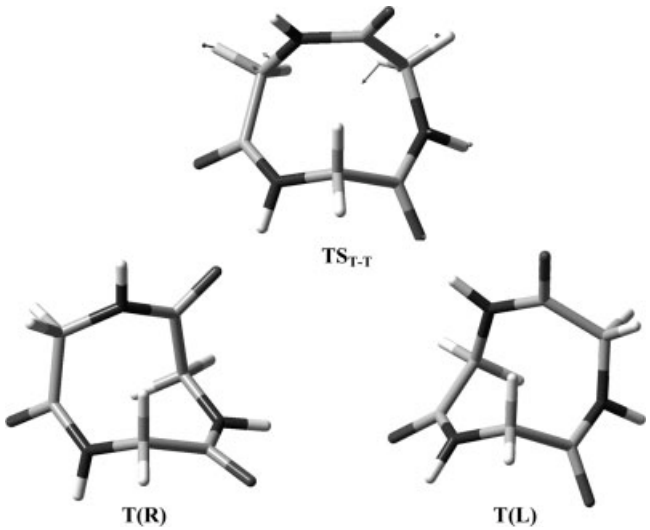

Figure 10. B3LYP/6-31G(d,p) optimized geometries of the T(R), $TS_{T\text{-}T}$ and T(L) forms of compound **III**. The vibrational modes are shown in the $TS_{T\text{-}T}$ transition state structure.

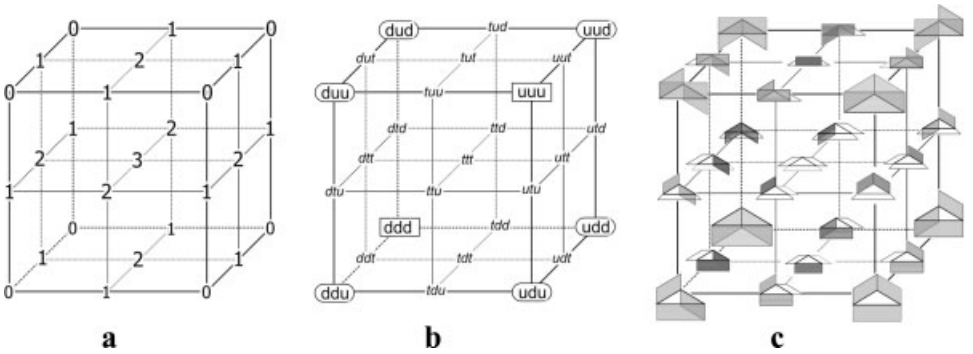

Figure 11. "Ideal" unit cell for compounds **I–III** coordinate space, showing (a) the location and types of critical points: (0) minima, (1) first order transition state, (2) second order transition states, (3) maxima. (b) Topological notation for the different critical points : u (up plane) , d (down plane) and t (transition state). (c) complete conformational hyperspace adopted by a system formed by a basic plane and three independent planes.

(compare Figs. 2 and 9). Once compound **III** adopts the $TS_{C\text{-}T}$ form, it is relaxed to the $TS_{T\text{-}T}$ form through the movement of only one methylene group (Fig. 9).

The general conformational behavior of **III** is very similar to that obtained for **I** and **II**. This is particularly interesting because in principle we can compare the conformational behavior of medium and large size peptides with that of the polyene analogues.

Topological Features of PEHS of Compounds I–III

A direct molecular geometry optimization is not much more than a nearly blind search for critical points on an exact, but unknown, potential energy hypersurface guided, or sometimes misguided, by chemical intuition. For conformational analysis, our chemical intuition is in general quite reliable although conceptually it does not go beyond the one-dimensional or single rotational case. Nature very often demands from us a multidimensional conformational analysis. This is the case of compounds **I–III** , which in principle is a multidimensional problem involving nine torsional modes. However, compounds **I** and **II** possess three *cis*-carbon–carbon double bonds and compound **III** possesses three *cis*-peptide bond; therefore, their conformational changes are governed mainly by six circular motions. To better understand the PEHSs of these compounds, it would be desirable to reduce the problem to a three-dimensional universe. Fortunately, in this case we can consider in principle only two levels of structural elements: (a) the plane determined by the three methylene groups and (b) the planes determined by each *cis*-double bond (in **I** and **II**) or each peptide bond (in **III**), which could be located up, down or in the same plane determined by the methylenes. Thus, we can obtain the different combinations of each plane as an independent variable determining a three-dimensional subspace where each dimension represents the relative position of each plane with respect to the plane determined by the methylenes.

Figure 11a shows the positions of the various critical points in a unit cell of the coordinates space. This figure represents a

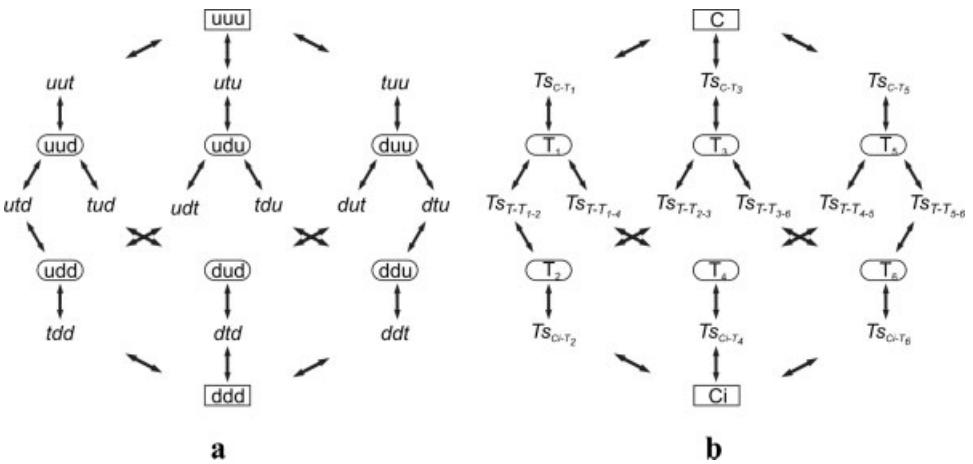

Figure 12. Schematic view for the conformational interconversion paths. Note that the degenerated TSs and Twist forms are denoted with different numbers in order to differentiate the alternative interconversion paths. The $TS_{T\text{-}T\ 1.3,\ 2\text{–}5,\ 4\text{–}6}$ are the opposite saddle forms of $TS_{T\text{-}T1.1\text{–}2,\ 3\text{–}4,\ 5\text{–}6}$.

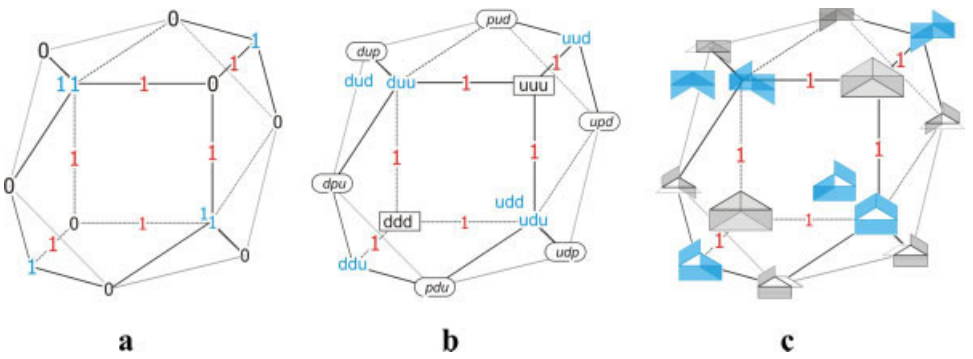

Figure 13. Unit cell for compounds **I–III** coordinate space, showing (a) the location and types of critical points: (0) minima, (1) first order transition state. (b) Topological notation for the different critical points : u (up plane) , d (down plane) and 1 (transition state). (c) schematic conformational hyperspace adopted by a system formed by a basic plane and three independent planes. [Color figure can be viewed in the online issue, which is available at www.interscience.wiley.com.]

general situation displaying the combinations of three independent variables (freedom degree). Note specially that there is a saddle point (**1**) between each pair of adjacent minima (**0**) and a super-saddle point (**2**) between each pair of adjacent saddle points (**1**). Saddle points may be interconnected either through minima or super-saddle points. In the centre of the unit cell the maximum (**3**) (for example a third order saddle point) is located, which is connected to the super-saddle points (second-order saddle points (**2**)) located in the centre of the faces. These critical points are connected with the first order saddle points (**1**) located in the centre of the awn grains, which interconnect the minima (**0**) located in the vertices of the unit cell. In Figure 11b we hypothesize that in the equilibrium structures, the planes are oriented up (u) or down (d) with respect to the methylenes plane. The up forms become down forms through TSs, which have been denoted with the letter "t". Figure 11c gives the complete conformational hyperspace adopted by a system formed by a basic plane and three independent planes. This figure allows us to visualize in a schematic form the positions assigned to the different critical points as well as the possible interconversion paths among the different critical points. These paths are schematized in Figure 12. In this figure we can observe that from each C form it is possible to obtain six twist forms using three equivalent paths. However, all the critical points possess degenerate forms, displaying two C forms, six T forms, six $TS_{C\text{-}T}$, and six $TS_{T\text{-}T}$ forms.

For the conformational interconversion of compounds **I–III**, the planes containing the double bonds (or peptide bonds) must be rotated through the restrictions imposed by the tetrahedron to the methylenes. Therefore, the interconversion process (to produce the inversion of the planes) may be carried out movement either one or two methylenes, as was observed in the conformational interconversion process (see previous section). As a direct consequence of the symmetry imposed to the molecular system, there is a recurrent symmetrical structure present in all the interconversion paths. This structure is the $TS_{T\text{-}T}$ form which possesses

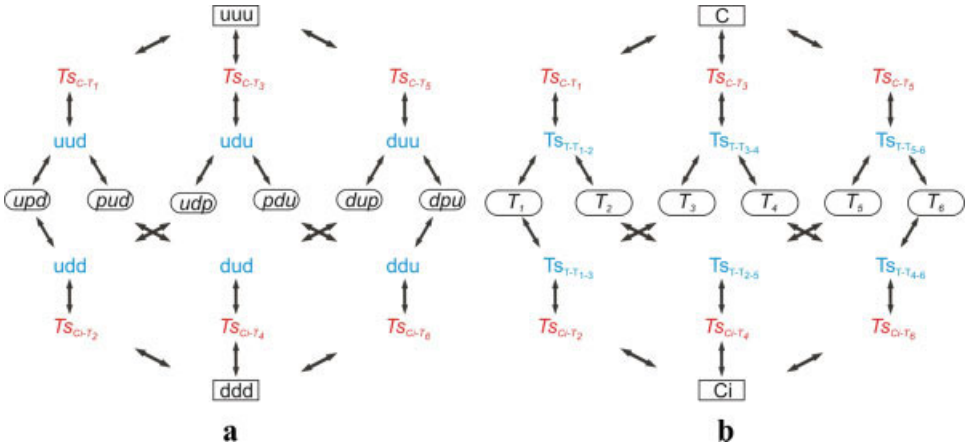

Figure 14. Schematic view for the conformational interconversion paths of compounds **I–III**. Note that the degenerated TSs and Twist forms are denoted with different numbers to differentiate the alternative interconversion paths. [Color figure can be viewed in the online issue, which is available at www.interscience.wiley.com.]

a very close pair of axial hydrogen atoms. This spatial ordering produces a steric repulsion, and therefore, it must be relaxed to adopt the twist form. This particular conformational profile gives a characteristic topological pattern as well. Thus, in the Crown-Twist interconversion, we can consider two steps: in the first one we obtain the TS $TS_{C\text{-}T}$ and then the symmetrical $TS_{T\text{-}T}$ form through the inversion of only one methylene while in the second step, this $TS_{T\text{-}T}$ form is relaxed to one of the next twist forms through the movement of two methylenes. It should be noted that the interconversion process between the global (C) and local (T) minimum involves two TSs with different characteristics ($TS_{C\text{-}T}$ and $TS_{T\text{-}T}$).

It is clear that the topological profile of compounds **I–III** is different to that shown in Figure 11. This is a direct consequence of the restrictions imposed by the symmetry as well as by the conformational mode in the interconversions between the PEHS critical points. In this case not all the regions of the cube shown in Figure 11 are available. Thus, the topological profile of compounds **I–III** is an adapted form of such ideal situation.

Figure 13a shows the topological indices for the interconversion process of the PEHS of compounds **I–III**. Figure 13b gives the different minima according to the orientation of the independent planes. Note that in the twist forms, one of the planes is coplanar with the methylene planes (denoted by sub-index p in this figure). Figure 13c in turn gives a schematic view of the most characteristic PEHS critical points.

Figure 14 shows the interconversion paths present in the PEHSs of compounds **I–III**. As was previously discussed, the C-T interconversion is carried out through two TSs.

Recently, we used a three-dimensional subspace strategy to depict the complex conformational (PEHS) intricacies of cyclononane.[4] Fortunately, the topological profiles of conformational PEHSs of compounds **I–III** are simpler than that reported for cyclononane. Although mathematically irrelevant, the topology of the PEHS of **I–III** is of considerable interest to visualize and better understand these hypersurfaces. The topology described earlier allows us to understand the conformational behavior of **I–III** where the torsion angles are interdependent. Thus, we may have a complete idea about the conformational intricacy of compounds **I–III.**

Conclusions

The exploration of a conformational energy hypersurface by methods that ignore all features other than local energy minima does not always give a satisfactory picture of the problem. It is desirable to determine, at least, the lowest energy TSs linking all pairs of conformations. In the present article the PEHSs of compounds **I–III** were investigated using theoretical calculations. *Ab initio* and DFT computations provide a clear picture for the conformational PEHS of these molecules from both structural and energetic points of view.

Altogether, four geometries (two minima and two TSs) were found to be important for a description of the conformational features of compounds **I–III**. B3LYP/aug-cc-pvdz//B3lYP/6-31G(d,p) predicts that the conformational interconversions between the crown and twist forms require 14.01, 26.71, and 17.79 kcal/mol for compounds **I**, **II,** and **III**, respectively, which is in agreement with the available experimental data. Theoretical calculations took into account all the conformational changes, allowing us to obtain a better idea about the conformational intricacies of the compounds PEHSs reported here.

Our results indicate that the general conformational behavior of cyclic peptide compounds is closely related to that of the cyclic polyene derivative possessing the same size ring. This is an interesting result because on the basis of the conformational behavior obtained for cyclic polyenes, it might be possible to estimate the general conformational intricacies of cyclic peptide compounds.

A topological analysis of the PEHSs is also reported here. The visualization of conformational hypersurfaces using a three-dimensional subspace strategy allows a rigorous analysis and detailed interpretation of the conformational phenomena. Thus, this model provides a logical explanation for the conformational intricacies of compounds **I–III**, a feature that is difficult to rationalize without a model, which allows visualization of the overall conformational problem.

Acknowledgments

R.D. Enriz is member of the Consejo Nacional de Investigaciones Científicas y Técnicas (CONICET-Argentina) staff.

References

1. Mierke, D. F.; Kurz, M.; Kessler, M. J. J Am Chem Soc 1994, 116, 1042.
2. Dygort, M.; Go. N.; Scheraga, H. A. Macromolecules 1975, 8, 750.
3. Lipton, M.; Still, W. C. J Comput Chem 1988, 9, 343.
4. Suvire, F. D.; Santágata, L. N.; Bombasaro, J. A.; Enriz, R. D. J Comput Chem 2006, 27, 188.
5. Winstein, S. J Am Chem Soc 1959, 81, 6524.
6. Radlick, P.; Winstein, W. J Am Chem Soc 1963, 85, 344.
7. Untch, K. G. J Am Chem Soc 1963, 85, 345.
8. Untch, K. G.; Kurtland, R. J. J Am Chem Soc 1963, 85, 346.
9. Roth, W. R.; Liebigs, J. Ann Chem 1964, 671, 10.
10. Roth, W. R.; Bang, W. B.; Goebel, P.; Sass, R. L.; Turner, R. B.; Yu, A. L. J Am Chem Soc 1964, 86, 3178.
11. Detty, M. R.; Paquette, L. A. Tetrahedron Lett 1977, 18, 347.
12. Untch, K. G.; Kurtland, R. J. J Mol Spectrosc 1964, 14, 156.
13. Anet, F. A. L.; Ghiachi, M. J Am Chem Soc 1980, 102, 2528.
14. Cookson, R. C.; Halton, B.; Stevens, D. R. J Chem Soc B 1969, 761.
15. Anad. M. K.; Cookson, R. C.; Stevens, D. R. J Am Chem Soc 1966, 88, 370.
16. Palmer, M. H.; Misber, J. D. J Mol Struct (Theochem) 1980, 67, 65.
17. Collet, A.; Gabard, J. J Org Chem 1980, 45, 5400.
18. Lesost, P.; Merlet, D. Sarfati, M.; Courtieu, J. Zimmerman, H.; Luz, Z. J Am Chem Soc 2002, 124, 10071.
19. Zimmerman, H.; Bader, V.; Poupko, R.; Wachtel, E.; Luz, Z. J Am Chem Soc 2002, 124, 15286.
20. Zimmerman, H.; Tolstoy, P.; Limbach, H. H.; Poupko, R.; Luz, Z. J Phys Chem B 2004, 103, 18772.
21. Lüttringhaus, A.; Peters, K. C. Angew Chem Int Ed Engl 1966, 5, 593.
22. Canceill, J.; Collet, A.; Gottarelli, G. J Am Chem Soc 1984, 106, 5997.
23. Burlinson, E.; Ripmeester, J. A. J Inclusion Phenom 1984, 1, 403.

24. Steed, J. W.; Zhang, H.; Atwood, J. L. Supramol Chem 1996, 7, 37.
25. Zimmerman, H.; Poupko, R.; Luz, Z.; Billard, J. Z. Naturforsch 1985, 40A, 149.
26. Malthête. J.; Collet, A. Nouv J Chim 1985, 9, 151.
27. Canceill, J.; Collet, A.; Gabard, J.; Gottarelli, G.; Spada, G. P. J Am Chem Soc 1985, 107, 1299.
28. Chakrabarti, A.; Chawla, H. M.; Hundal, G.; Pant, N. Tetrahedron 2005, 61, 12323.
29. Collet, A. Tetrahedron 1987, 43, 5725.
30. Dale, J.; Titlestad, K. J Chem Soc D Chem Commun 1969, 12, 656.
31. Titlestad, K. Acta Chem Scand B 1975, 29, 153.
32. Groth, P. Acta Chem Scand A 1976, 30, 838.
33. Hioki, H.; Kinami, H.; Yoshida, A.; Kojima, A.; Kodama, M.; Takaoka, S.; Veda, K.; Katsu, T. Tetrahedron Lett 2004, 45, 1091.
34. Hendrickson, J. B. J Am Chem Soc 1964, 86, 7047.
35. Anet, F. A. L. Top Curr Chem 1974, 45, 169.
36. Dale, J. Top Stereochem 1976, 9, 199.
37. Frisch, M. J.; Trucks, G. W.; Schlegel, H. B.; Scuseria, G. E.; Robb, M. A.; Cheeseman, J. R.; Montgomery, J. A., Jr.; Vreven, T.; Kudin, K. N.; Burant, J. C.; Millam, J. M.; Iyengar, S. S.; Tomasi, J.; Barone, V.; Mennucci, B.; Cossi, M.; Scalmani, G.; Rega, N.; Petersson, G. A.; Nakatsuji, H.; Hada, M.; Ehara, M.; Toyota, K.; Fukuda, R.; Hasegawa, J.; Ishida, M.; Nakajima, T.; Honda, Y.; Kitao, O.; Nakai, H.; Klene, M.; Li, X.; Knox, J. E.; Hratchian, H. P.; Cross, J. B.; Adamo, C.; Jaramillo, J.; Gomperts, R.; Stratmann, R. E.; Yazyev, O.; Austin, A. J.; Cammi, R.; Pomelli, C.; Ochterski, J. W.; Ayala, P. Y.; Morokuma, K.; Voth, G. A.; Salvador, P.; Dannenberg, J. J.; Zakrzewski, V. G.; Dapprich, S.; Daniels, A. D.; Strain, M. C.; Farkas, O.; Malick, D. K.; Rabuck, A. D.; Raghavachari, K.; Foresman, J. B.; Ortiz, J. V.; Cui, Q.; Baboul, A. G.; Clifford, S.; Cioslowski, J.; Stefanov, B. B.; Liu, G.; Liashenko, A.; Piskorz, P.; Komaromi, I.; Martin, R. L.; Fox, D. J.; Keith, T.; Al-Laham, M. A.; Peng, C. Y.; Nanayakkara, A.; Challacombe, M.; Gill, P. M. W.; Johnson, B.; Chen, W.; Wong, M. W.; Gonzalez, C. and Pople, J. A. Gaussian 03, Revision B.05 2003, Gaussian, Inc., Pittsburgh PA.
38. (a) Santagata, L. N.; Suvire, F. D.; Enriz, R. D.; Torday, J. L.; Csizmadia, I. G. J Mol Struct (Theochem) 1999, 465, 33; (b) Santagata, L. N.; Suvire, F. D.; Enriz, R. D. J Mol Struct (Theochem) 2000, 507, 89; (c) Santagata, L. N.; Suvire, F. D.; Enriz, R. D. J Mol Struct (Theochem) 2001, 536, 173; (d) Santagata, L. N.; Suvire, F. D.; Enriz, R. D. J Mol Struct (Theochem) 2001, 571, 91.
39. Gonzalez, C.; Schlegel, H. B. J Chem Phys 1989, 90, 2154.
40. Gonzalez, C.; Schlegel, H. B. J Phys Chem 1990, 94, 5523.
41. Russo, T. V.; Martin, R. L.; Hay, P. J. J Phys Chem 1995, 99, 17085.
42. Ignaczak, A.; Gomez, J. A. N. F. Chem Phys Lett 1996, 257, 609.
43. Cotton, F. A.; Feng, X. J Am Chem Soc 1997, 119, 7514.
44. Lee, C.; Yang, W.; Parr, R. G. Phys Rev 1988, 37, 785.
45. Miehlich, B.; Savin, A.; Stoll, H.; Preuss, M. Chem Phys Lett 1989, 157, 200.
46. Becke, A. Phys Rev A 1988, 38, 3098.
47. Becke, A. J Chem Phys 1993, 98, 5648.
48. Ardebill, M. H. P.; Dougherty, D. A.; Misiow, K.; Schwartz, L. H. J Am Chem Soc 1978, 100, 7994.
49. Dougherty, D. A.; Hounshell, W. D.; Schlegel, H. B.; Bell, R. A.; Misiow, K. Tetrahedron Lett 1976, 17, 3479.
50. Dougherty, D. A.; Schlegel, H. B.; Misiow, K. Tetrahedron 1978, 34, 1441.
51. Mezey, P. G. In Progress in Theoretical Organic Chemistry, Vol. 2: Applications of MO Theoretical in Organic Chemistry; Csizmadia, I. G., Ed.; Elsevier: Amsterdam, 1977; pp. 127–161.
52. Metiu, H.; Ross, J.; Silbey, R.; George, T. F. J Chem Phys 1974, 61, 3200.
53. Valtazanos, P.; Ruedenberg, K. Theor Chim Acta 1986, 69, 281.
54. Singleton, D. A.; Hang, C.; Szymanski, M. J.; Meyer, M. P.; Leach, A. G.; Kuwata, K. T.; Chen, J. S.; Greer, A.; Foote, C. S.; Houk, K. N. J Am Chem Soc 2003, 125, 1319.
55. Gonzalez-Lafont, A.; Moreno, M.; Lluch, J. M. J Am Chem Soc 2004, 126, 13089.
56. Wei, H.; Hrovat, D. A.; Borden, W. T. J Am Chem Soc 2006, 128, 16676.